J|A|C|S
ARTICLES
Published on Web 07/23/2002

Spin-State Alteration from Sterically Enforced Ligand Rotation in Bis(indenyl)chromium(II) Complexes[1]

Erik D. Brady,[†] Jason S. Overby,[†] M. Brett Meredith,[†] Adam B. Mussman,[†] Michael A. Cohn,[†] Timothy P. Hanusa,*[,†] Gordon T. Yee,[‡,||] and Maren Pink[§]

Contribution from the Department of Chemistry, Vanderbilt University, Nashville, Tennessee 37235, Department of Chemistry & Biochemistry, University of Colorado, Boulder, Colorado 80309, and X-ray Crystallographic Laboratory, Chemistry Department, University of Minnesota, Minneapolis, Minnesota 55455

Received October 19, 2001

Abstract: The rotational orientation of cyclopentadienyl rings usually has no effect on d-orbital energy levels and splitting in transition metal complexes. With related but less symmetrical carbocyclic ligands, however, the magnetic properties of the associated complexes can be altered by the alignment of the ligands. Examples of this effect are found in substituted organochromium(II) bis(indenyl) complexes. The monosubstituted compounds $(1\text{-}RC_9H_6)_2Cr$ (R = *t*-Bu, $SiMe_3$) are prepared from the substituted lithium indenides and $CrCl_2$ in THF; they are high-spin species with four unpaired electrons. Their spin state likely reflects that in the unknown monomeric $(C_9H_7)_2Cr$, which is calculated to have a high-spin ($S = 2$) ground state in the staggered configuration (180° rotation angle). However, the analogous bis(indenyl) complexes containing *t*-Bu or $SiMe_3$ groups in both the 1 and 3 positions on the indenyl ligands ($(1,3\text{-}R_2C_9H_5)_2Cr$) are *low*-spin compounds with two unpaired electrons. X-ray diffraction results indicate that $[1\text{-}(t\text{-}Bu)C_9H_6]_2Cr$ exists in a staggered conformation, with Cr−C (av) = 2.32(4) Å. In contrast, the average Cr−C distances in $[1,3\text{-}(t\text{-}Bu \text{ or } SiMe_3)_2C_9H_5]_2Cr$ are 2.22(2) and 2.20(2) Å, respectively, and the rings are in a gauche configuration, with rotation angles of 87°. The indenyl conformations are sterically imposed by the bulk of the *t*-Bu and $SiMe_3$ substituents. The change from a staggered to a gauche indenyl orientation lowers the symmetry of a $(C_9H_7)_2M$ complex and allows greater mixing of metal and ligand orbitals. Calculations indicate that previously nonbonding π orbitals of the indenyl anion are able to interact with the chromium d orbitals, producing bonding and antibonding combinations. The latter remain unpopulated, and the resulting increase in the HOMO−LUMO gap forces the complexes to adopt a low-spin configuration. The possibility of using sterically imposed ligand rotation as a means of spin-state manipulation makes indenyl compounds a potentially rich source of magnetically adjustable molecules.

Introduction

There is considerable interest in the synthesis of transition metal compounds that have specifically tailored magnetic properties.[2] Metallocene-based complexes have been particularly attractive in this regard, and variations in the metals, their oxidation states, and ring substituents have led to a variety of species displaying spin-crossover behavior,[3,4] molecular ferromagnetism,[5−9] and ferromagnetic/antiferromagnetic exchange.[10]

The control over magnetic properties that is possible in metallocenes is perhaps best illustrated by manganocene, Cp_2Mn, and its ring-substituted derivatives. The parent compound is high spin ($S = {}^5/_2$; $\mu_B = 5.50$) at 373 K but converts to a low-spin species ($S = {}^1/_2$; $\mu_B = 1.99$) at lower temperatures (193 K).[11] Alkylation of the cyclopentadienyl ring increases the d-orbital splitting and preference for spin pairing, so that Cp^*_2Mn ($Cp^* = C_5Me_5$), for example, is low spin ($\mu_B = 2.18$) over a large temperature range.[12] Interestingly, however, the octaisopropylated derivative $[C_5(i\text{-}Pr)_4H]_2Mn$ is a *high*-spin molecule ($\mu_B{}^{200K} = 5.73$) even though the isopropyl groups on

* To whom correspondence should be addressed. E-mail: t.hanusa@vanderbilt.edu.
[†] Vanderbilt University.
[‡] University of Colorado.
[§] University of Minnesota.
[||] Current address: Department of Chemistry, Virginia Tech, Blacksburg, VA 24061.

(1) Presented in part at the 221st Meeting of the American Chemical Society, San Diego, CA, April 2001; paper INOR 623.
(2) Gütlich, P.; Hauser, A.; Spiering, H. *Angew. Chem., Int. Ed. Engl.* **1994**, *33*, 2024−2054.
(3) Koehler, F. H.; Schlesinger, B. *Inorg. Chem.* **1992**, *31*, 2853−2859.
(4) Cozak, D.; Gauvin, F.; Demers, J. *Can. J. Chem.* **1986**, *64*, 71−75.
(5) Yee, G. T.; Manriquez, J. M.; Dixon, D. A.; McLean, R. S.; Groski, D. M.; Flippen, R. B.; Narayan, K. S.; Epstein, A. J.; Miller, J. S. *Adv. Mater.* **1991**, *3*, 309−311.
(6) Miller, J. S.; Vazquez, C.; McLean, R. S.; Reiff, W. M.; Aumueller, A.; Huenig, S. *Adv. Mater. (Weinheim, Fed. Repub. Ger.)* **1993**, *5*, 448−450.
(7) O′Hare, D.; Brookes, J.; Watkin, D. J. *J. Mater. Chem.* **1991**, *1*, 691−697.
(8) Yee, G. T.; Whitton, M. J.; Sommer, R. D.; Frommen, C. M.; Reiff, W. M. *Inorg. Chem.* **2000**, *39*, 1874−1877.
(9) Kaul, B. B.; Durfee, W. S.; Yee, G. T. *J. Am. Chem. Soc.* **1999**, *121*, 6862−6866.
(10) Hilbig, H.; Hudeczek, P.; Koehler, F. H.; Xie, X.; Bergerat, P.; Kahn, O. *Inorg. Chem.* **1998**, *37*, 4246−4257.
(11) Switzer, M. E.; Wang, R.; Rettig, M. F.; Maki, A. H. *J. Am. Chem. Soc.* **1974**, *96*, 7669−7674.
(12) Robbins, J. L.; Edelstein, N.; Spencer, B.; Smart, J. C. *J. Am. Chem. Soc.* **1982**, *104*, 1882−1893.

10.1021/ja012390a CCC: $22.00

the cyclopentadienyl rings should strengthen the ligand field. In this case, interligand steric crowding forces the cyclopentadienyl rings to move away from the metal center; the longer M−L distances weaken the ligand field and stabilize the high-spin state.[13,14] Addition of a trimethylsilyl group to each Cp ring can stabilize the high-spin state also, but here the origin of the effect seems to be electronic, as there is no obvious crowding in the structure of $[C_5(SiMe_3)H_4]_2Mn$.[15]

In none of the complexes mentioned above is the *rotational* conformation of the cyclopentadienyl ligands used to rationalize their effects on d-orbital energy levels and splitting. Although sterically bulky substituents can enforce a particular arrangement (e.g., $[C_5(i\text{-}Pr)_3H_2]_2Mn$ adopts a staggered conformation to avoid undue intramolecular crowding[13]), molecular orbital analysis of linear metallocenes (Cp'_2M) can be done equally well under eclipsed (D_{5h}) or staggered (D_{5d}) symmetry.[16] Similarly, the fact that the corresponding bent complexes have different symmetry (C_{2v} or C_s, respectively) is also not critical to understanding the changes in orbital energies that accompany bending.[17] Furthermore, in mono(cyclopentadienyl) complexes such as $CpML_3$ (M = Cr, Mo), the orientation of the cyclopentadienyl ring has been shown not to alter the calculated total energy of the molecules.[18−20]

With less inherently symmetrical ligands, however, differences in orientation can become important. The indenyl ligand, for instance, is frequently considered to be an analogue of the cyclopentadienyl ring,[21,22] but its nodal properties are somewhat different from those of the Cp^- anion (Figure 1). In addition, bis(indenyl)metal complexes can display metal-dependent conformational differences; e.g., the ligands in Ind_2Fe ($Ind = C_9H_7$) are eclipsed,[23] whereas those in Ind_2Ni are staggered and noticeably slipped from symmetrical η^5-coordination (Ni−C distances range from 1.97 to 2.48 Å). The differences have been traced to the electron count in the complexes (20 e^- (Ni) vs 18 e^- (Fe)); antibonding orbitals that would be occupied in an eclipsed configuration in the nickel complex remain empty in a staggered arrangement.[24]

The dependence of ligand conformation on orbital occupancy makes bis(indenyl) complexes attractive platforms for studying the interaction between electronic and steric effects on d-orbital splitting and magnetic properties. In the search for indenyl-based systems that would be amenable to spin-state manipulation, we have been interested in the possibilities provided by chromium(II) compounds. Bis(indenyl)chromium itself is a dimer, $[Ind_2Cr]_2$,[25] but permethylation produces a low-spin ($S = 1$) monomer, Ind^*_2Cr ($Ind^* = C_9(CH_3)_7$), with a staggered geometry.[26] Curiously, however, the bis(diisopropyl)indenyl complex $(Ind^{2i})_2Cr$ (Ind^{2i} = 1,3-(i-Pr)$_2C_9H_5$) is a *high*-spin ($S = 2$) monomer, also with a staggered configuration.[27] There is no crystallographic evidence for steric congestion in the molecule that would favor this spin state, as occurs in $[C_5(i\text{-}Pr)_4H]_2Mn$. The high-spin state of $(Ind^{2i})_2Cr$ could be explained, however, if the magnetic ground state of the (unknown) staggered Ind_2Cr monomer were also high spin. This assumption, which is supported by calculations,[28] would then imply that the role of the isopropyl groups in $(Ind^{2i})_2Cr$ is structural; i.e., they block the dimerization that occurs in the absence of any indenyl substituents, without altering the inherent high-spin state of the monomer. If this interpretation is correct, the low-spin state of Ind^*_2Cr can then be understood as a result of the enhanced electron richness of the permethylated indenyl ring and the consequent increase in d-orbital splitting.

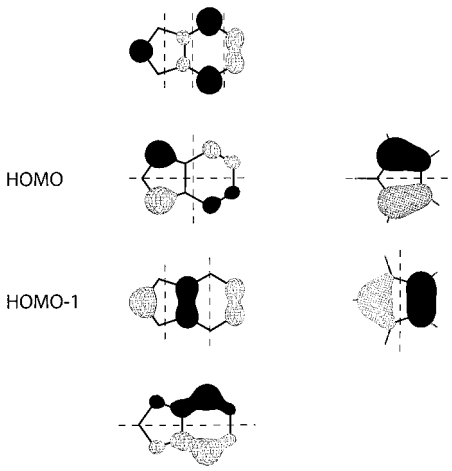

Figure 1. Frontier π orbitals of the indenyl and cyclopentadienyl anions (left and right, respectively). Although the nodal properties of the HOMO and HOMO-1 for both anions are similar, there is negligible electron density on the bridgehead carbons of the five-membered ring in the HOMO of the indenyl anion.

Bis(indenyl)chromium(II) complexes thus have two properties that should make them amenable to manipulation of their magnetic behavior: (1) the ready accessibility of two spin states (triplet and quintet) for the metal center and (2) the known sensitivity of Ind_2M frameworks to orientation-dependent orbital effects. As in metallocene complexes, sterically bulky substituents can alter the orientation of indenyl ligands; unlike the eclipsed Ind_2Fe, for example, the diamagnetic (+)-bis(η^5-2-menthylindenyl)iron(II) has a rotation angle of 134°, attributed to intramolecular steric congestion with the terpene groups.[29]

(13) Hays, M. L.; Burkey, D. J.; Overby, J. S.; Hanusa, T. P.; Yee, G. T.; Sellers, S. P.; Young, V. G., Jr. *Organometallics* **1998**, *17*, 5521−5527.
(14) Sitzmann, H.; Schär, M.; Dormann, E.; Keleman, M. *Z. Anorg. Allg. Chem.* **1997**, *623*, 1609−1613.
(15) Hebendanz, N.; Köhler, F. H.; Müller, G.; Riede, J. *J. Am. Chem. Soc.* **1986**, *108*, 3281−3289.
(16) Cotton, F. A. *Chemical Applications of Group Theory*, 3rd ed.; John Wiley & Sons: New York, 1990.
(17) Green, J. C. *Chem. Soc. Rev.* **1998**, *27*, 263−272.
(18) Legzdins, P.; McNeil, W. S.; Smith, K. M.; Poli, R. *Organometallics* **1998**, *17*, 615−622.
(19) Cacelli, I.; Keogh, D. W.; Poli, R.; Rizzo, A. *J. Phys. Chem. A* **1997**, *101*, 9801−9812.
(20) Cacelli, I.; Keogh, D. W.; Poli, R.; Rizzo, A. *New J. Chem.* **1997**, *21*, 133−135.
(21) Cauletti, C.; Green, J. C.; Kelly, M. R.; Powell, P.; Van Tilborg, J.; Robbins, J.; Smart, J. *J. Electron Spectrosc. Relat. Phenom.* **1980**, *19*, 327−353.
(22) Evans, S.; Green, M. L. H.; Nagy, A.; Stringer, G. *J. Chem. Soc., Faraday Trans. 2* **1972**, 1847−1865.
(23) The rotation angle is defined as in ref 26; i.e., the angle formed by the intersection of the two planes determined by the centroids of the five- and six-membered rings.
(24) Calhorda, M. J.; Veiros, L. F. *Coord. Chem. Rev.* **1999**, *185−186*, 37−51.
(25) Heinemann, O.; Jolly, P. W.; Krüger, C.; Verhovnik, G. P. J. *Organometallics* **1996**, *15*, 5462−5463.
(26) O′Hare, D.; Murphy, V. J.; Kaltsoyannis, N. *J. Chem. Soc., Dalton Trans.* **1993**, 383−392.
(27) Overby, J. S.; Hanusa, T. P.; Sellers, S. P.; Yee, G. T. *Organometallics* **1999**, *18*, 3561−3562.
(28) The original estimate of a 21 kcal mol^{-1} difference between the high-spin and low-spin states of Ind_2Cr (ref 27) was based on semiempirical PM3(tm) methods. This number has been lowered with DFT calculations to 8.9 kcal mol^{-1} (geometry optimization and frequency calculations performed with staggered symmetry) (approximately C_i, although none was imposed) and the B3PW91 functional, the 6-31+G(d) basis set for geometry optimization and the 6-311+G(2d, 2p) basis set for final energy calculations on Cr, C, and H. Both $S = 1$ and $S = 2$ geometries are minimums on their potential energy surfaces ($N_{imag} = 0$).
(29) Schumann, H.; Stenzel, O.; Dechert, S.; Halterman, R. L. *Organometallics* **2001**, *20*, 1983−1991.

If substituents were used to alter the rotation of the ligands relative to the metal center on a chromium(II) complex, however, the induction of specific magnetic behavior becomes a possibility. We describe here the effects of such substitution in various substituted bis(indenyl)chromium(II) species.

Experimental Section

General Considerations. Unless mentioned otherwise, all manipulations were performed with the rigorous exclusion of air and moisture using high-vacuum, Schlenk, or glovebox techniques. Proton and carbon (^{13}C) NMR spectra were obtained on a Bruker DPX-300 at 300 and 75.5 MHz, respectively, and were referenced to the residual proton and ^{13}C resonances of $CDCl_3$ (δ 7.26 and 77.2). Elemental analyses were performed by Desert Analytics (Tucson, AZ); despite repeated analysis, some compounds analyzed low in carbon by up to 1%. Infrared data were obtained on an ATI Mattson-Genesis FT-IR spectrometer as neat solutions or as KBr pellets prepared as previously described.[30] Melting points were determined on a Laboratory Devices Mel-Temp apparatus in sealed capillaries. Mass spectra were obtained using a Hewlett-Packard 5890 Series II gas chromatograph/mass spectrometer.

Materials. Nominally anhydrous chromium(II) chloride (Aldrich) was heated under vacuum (150 °C, 10^{-4} Torr) to ensure complete removal of coordinated water. Indene (Acros) was distilled prior to use. Chlorotrimethylsilane, *tert*-butyl bromide, potassium bis(trimethylsilyl)amide, ammonium chloride, and anhydrous magnesium sulfate were purchased from Aldrich or Acros and used as received. *n*-BuLi was purchased from Aldrich as a 2.5 M solution in hexanes and used as received. Celite 521 and glass wool were thoroughly heated and stored under nitrogen prior to use. THF, toluene, and hexanes were distilled under nitrogen from potassium benzophenone ketyl.[31] $CDCl_3$ was purchased from Aldrich and dried with 4A molecular sieves prior to use. Toluene-d_8 was vacuum distilled from Na/K (22/78) alloy and stored over 4A molecular sieves prior to use.

Magnetic Measurements. Variable-temperature solution magnetic susceptibility data were obtained in toluene-d_8 on a Bruker DRX-400 spectrometer using the Evans' NMR method.[32−35] Solid-state magnetic susceptibility data were measured on a 5 T Quantum Design MPMS-5 SQUID magnetometer. To handle the extremely air-sensitive compounds, the previously described sample holder was used;[13] the diamagnetic susceptibility of the sample holder was accepted as the average value of the measurements on several identical sample holders. The diamagnetic correction for each complex was estimated from Pascal's constants.

Synthesis of 1-Mono- and 1,3-Di(*tert*-butyl)indene, 1-(*t*-Bu)C_9H_7 (HInd^{1T}) and 1,3-(*t*-Bu)$_2C_9H_6$ (HInd^{2T}). A 1-L, three-necked flask was charged with hexanes (400 mL) and indene (15.3 mL, 131 mmol); after the mixture was cooled in an ice bath, dropwise addition of *n*-BuLi (52.5 mL, 131 mmol) led to the immediate formation of lithium indenide. Stirring was maintained as the solution warmed to room temperature. After 8 h, *tert*-butyl bromide (15.1 mL, 0.131 mol) was slowly added via a second addition funnel. The resulting mixture was refluxed overnight, after which it was cooled, poured into a dilute solution of NH_4Cl, and stirred. The aqueous layer was separated and washed twice with small amounts (20 mL) of hexanes. The hexanes layers were combined, dried with anhydrous $MgSO_4$, and transferred to a second 1-L, three-necked flask.

Under a positive pressure of nitrogen, *n*-BuLi (53.0 mL, 131 mmol) was added dropwise at 0 °C. The solution was refluxed for 2 h and again cooled to 0 °C. *tert*-Butyl bromide (~16 mL, 130 mmol) was added, and the solution was refluxed for 4 h. The mixture was then poured into a dilute solution of NH_4Cl and stirred. The hexanes layer was isolated and dried over $MgSO_4$. The aqueous layer was washed with hexanes (2 × 15 mL). The hexane extract was dried and combined with the previously isolated hexanes layers.

The combined solution was reduced to ~15 mL and then transferred to a silica gel column (45 mm × 500 mm). HInd^{1T} and HInd^{2T} were extracted simultaneously with hexanes as an orange band. The mixture was purified by vacuum distillation at 200 mTorr; HInd^{1T} distilled at 52 °C (7.74 g, 34%) and HInd^{2T} distilled at 61 °C (3.36 g, 11%). The spectra of HInd^{1T} (^{1}H NMR and GC/MS) were compared with literature values[36,37] prior to further use. HInd^{2T} has not been previously reported. ^{1}H NMR ($CDCl_3$): δ 8.05 (doublet, J = 7.0 Hz, 2H, C_6 ring-Ind); 7.65 (doublet, J = 6.6 Hz, 2H, C_6 ring-Ind); 7.35 (multiplet, 1H, C_5 ring-Ind); 7.32 (multiplet, 1H, C_5 ring-Ind); 1.55 (singlet, 18H, *t*-Bu). ^{13}C NMR ($CDCl_3$): δ 158.1 (Ind); 142.3 (Ind); 139.1 (Ind); 138.6 (Ind); 127.4 (Ind); 125.0 (Ind); 122.5 (Ind); 121.4 (Ind); 33.7 ($C(CH_3)_2$); 29.5 ($C(CH_3)_3$). Principal IR bands (cm^{-1}): 2979 (w), 2966 (s), 2940 (w), 2927 (s), 2882 (w), 2856 (w), 1459 (m), 1445 (m), 1366 (m), 1345 (m), 1268 (w), 1202 (w), 1157 (w), 815 (w), 795 (s). MS (EI) *m*/*z*: 228 (M^+), 172 ($M^+ - t$-Bu), 116 ($M^+ - 2\ t$-Bu), 57 (M^+ − Ind, *t*-Bu).

Synthesis of 1-Mono- and 1,3-Bis(trimethylsilyl)indene, 1-(Si(CH$_3$)$_3$)C_9H_7 (HInd^{1Si}) and 1,3-(Si(CH$_3$)$_3$)$_2C_9H_6$ (HInd^{2Si}). In a procedure similar to that employed for the *tert*-butylindenes, indene (49.0 mL, 420 mmol) was allowed to react with *n*-BuLi (169 mL, 0.423 mol) at 0 °C. After 6 h, chlorotrimethylsilane (56.0 mL, 441 mmol) was slowly added, and the resulting slurry was refluxed overnight. Standard workup was used to isolate HInd^{1Si}.

To a stirring solution of HInd^{1Si}, *n*-BuLi (169 mL, 423 mmol) was added dropwise at 0 °C. The solution was refluxed for 2 h and then cooled again to 0 °C. Chlorotrimethylsilane (56.0 mL, 441 mmol) was added, and the solution was then refluxed for 5 h. Workup as with the *tert*-butyl derivatives afforded HInd^{1Si} and HInd^{2Si} as coeluates from column chromatography. The mixture was purified by vacuum distillation at 150 mTorr; HInd^{1Si} distilled at 55 °C (25.2 g, 43%) and HInd^{2Si} distilled at 79 °C (14.8 g, 14%). Both HInd^{1Si} and HInd^{2Si} are known compounds, and their purities were confirmed by comparison of spectra (^{1}H NMR and GC/MS) prior to further use.[37]

Synthesis of Bis(1-*tert*-butylindenyl)chromium(II), (Ind^{1T})$_2$Cr. HInd^{1T} (8.00 g, 46.4 mmol) was converted into its lithium salt by reaction with *n*-BuLi (18.6 mL) in 200 mL of hexanes at 0 °C. After the mixture was stirred overnight, isolation of the precipitate by filtration, washing with hexanes (2 × 15 mL), and drying under vacuum yielded 5.61 g (68%) of an ivory-colored solid.

A Schlenk flask was charged with 0.362 g (2.03 mmol) of the lithium indenide, to which was added 30 mL of THF. The solution was added dropwise with a cannula into a THF slurry of $CrCl_2$ (0.125 g, 1.02 mmol) that had been cooled to −78 °C. The solution immediately turned deep green and was allowed to stir for 2 h. On being warmed to room temperature, the solution turned purple, and removal of THF under vacuum left a purple solid. Hexanes (25 mL) was added to the residue, and the extract was filtered and placed in a freezer overnight. The following day, a large amount of (Ind^{1T})$_2$Cr had precipitated as a crystalline solid. Additional material was obtained by evaporating the solvent from mother liquor under vacuum to a powder. The crystals and powder were found to total 0.327 g (82% yield). Characterization of the crystals: mp 150 °C (dec). Anal. Calcd for $C_{26}H_{30}Cr$: C, 79.16; H, 7.66. Found: C, 78.24; H, 7.67. Principal IR bands (cm^{-1}): 2927 (s), 2815 (m), 2787 (m), 2672 (w), 1483 (m), 1391 (m). Solution magnetic moment (μ (T (K)): 4.97 (203), 5.01 (213), 4.94 (223), 4.88 (233), 4.83 (243), 4.78 (253), 4.74 (263), 4.69 (273), 4.63 (283).

(30) Williams, R. A.; Tesh, K. F.; Hanusa, T. P. *J. Am. Chem. Soc.* **1991**, *113*, 4843−4851.
(31) Perrin, D. D.; Armarego, W. L. F. *Purification of Laboratory Chemicals*, 3rd ed.; Pergamon: Oxford, 1988.
(32) Evans, D. F. *J. Chem. Soc.* **1959**, 2003−2005.
(33) Grant, D. H. *J. Chem. Educ.* **1995**, *72*, 39−40.
(34) O'Hare, D.; Green, J. C.; Marder, T.; Collins, S.; Stringer, G.; Kakkar, A. K.; Kaltsoyannis, N.; Kuhn, A.; Lewis, R.; Mehnert, C.; Scott, P.; Kurmoo, M.; Pugh, S. *Organometallics* **1992**, *11*, 48−55.
(35) Sur, S. K. *J. Magn. Reson.* **1989**, *82*, 169−173.
(36) Cedheim, L.; Eberson, L. *Synthesis* **1973**, 159.
(37) Ready, T. E.; Chien, J. C. W.; Rausch, M. D. *J. Organomet. Chem.* **1999**, *583*, 11−27.

Synthesis of Bis(1,3-di(*tert*-butyl)indenyl)chromium(II), $(Ind^{2T})_2Cr$. $HInd^{2T}$ (6.89 g, 30.1 mmol, dissolved in 35 mL of hexanes) was converted into its potassium salt by reaction with $K[N(SiMe_3)_2]$ (6.02 g, 30.2 mmol) dissolved in toluene (40 mL). When the solutions were combined, the mixture immediately turned black. After the reaction was stirred overnight, a brown precipitate was isolated by filtration, washed twice with hexanes (25 mL), and dried under vacuum to yield 4.81 g (60%) of a light yellow solid.

$CrCl_2$ (0.100 g, 0.814 mmol) and the potassium indenide (0.434 g, 1.63 mmol) were placed in a flask equipped with a stirring bar. A dark red solution immediately formed on the addition of 40 mL of THF. After the mixture was stirred overnight, the solvent was removed under vacuum to leave a dark red solid. Hexanes (20 mL) was added, and insoluble impurities were removed by filtration through glass wool and Celite 521. The solvent was removed from the brick red filtrate by slow evaporation; after 12 h, large needle-shaped crystals were isolated by decanting the remaining mother liquor. The solvent was evaporated from the latter under vacuum to afford additional solid as a powder (0.145 g, 35% yield). Characterization of the crystals: mp 278−280 °C. Anal. Calcd for $C_{34}H_{46}Cr$: C, 80.59; H, 9.15. Found: C, 80.41; H, 9.24. Solution magnetic moment (μ (T (K)): 2.91 (182), 2.94 (192.8), 2.98 (202.1), 3.03 (212.7), 3.08 (222.2), 3.15 (232.8), 3.22 (243.2), 3.30 (253.4), 3.37 (264), 3.42 (273), 3.46 (280), 3.51 (290), 3.55 (300.5), 3.57 (310), 3.61 (320), 3.63 (330), 3.65 (340), 3.64 (350).

Synthesis of Bis[1-trimethylsilylindenyl]chromium(II), $(Ind^{1Si})_2Cr$. As in the preparation of the lithium salt of $HInd^{1T}$, $HInd^{1Si}$ (7.26 g, 38.5 mmol) and *n*-BuLi (15.4 mL, 38.5 mmol) were combined in hexanes (100 mL) and stirred overnight in a Schlenk flask. Isolation of the resulting precipitate by filtration, washing twice with hexanes (15 mL), and drying under vacuum yielded 5.56 g (74%) of a light pink solid.

$CrCl_2$ (0.125 g, 1.02 mmol) and the lithium indenide (0.395 g, 2.03 mmol) were placed in a flask equipped with a stirring bar. THF (40 mL) was added, which produced a dark green solution. After the mixture was stirred overnight, the solvent was removed under vacuum to leave a purple solid. Hexanes (20 mL) was added, and insoluble impurities were removed by filtration over a medium-porosity glass frit. The filtrate was cooled in a freezer; after 6 h, small purple crystals of $(Ind^{1Si})_2Cr$ had appeared. Once no additional crystal growth was observed, the mother liquor was removed by cannulation and evaporated under vacuum to afford additional material. Total yield: 0.302 g (70%). Characterization of the crystals: mp 164−165 °C. Anal. Calcd for $C_{24}H_{30}CrSi_2$: C, 67.56; H, 7.09. Found: C, 66.96; H, 7.10. Principal IR bands (cm^{-1}): 3045−2805 (s), 2673 (m), 1478 (m), 1447 (m), 1351 (m), 1305 (w), 1136 (w), 1064 (w), 1037 (w), 903 (w), 730 (m). Solution magnetic moment (μ (T (K)): 5.03 (183), 5.03 (193), 5.01 (203), 5.01 (213), 4.99 (223), 4.99 (233), 5.03 (243), 5.00 (253), 4.97 (263), 4.93 (273), 4.93 (283), 4.89 (298).

Synthesis of Bis[1,3-bis(trimethylsilyl)indenyl]chromium(II), $(Ind^{2Si})_2Cr$. As in the preparation of the potassium salt of $HInd^{2T}$, $HInd^{2Si}$ (8.0 g, 31 mmol) and $K[N(SiMe_3)_2]$ (6.12 g, 30.7 mmol) were combined in a mixture of toluene and hexanes (70 mL). The following day, a tan precipitate was separated by filtration over a medium-porosity glass frit. The precipitate was washed with hexanes (2 × 25 mL) and dried thoroughly under vacuum to afford 5.87 g (64%) of a tan solid.

$CrCl_2$ (0.062 g, 0.51 mmol) and the potassium indenide were placed in a flask equipped with a stirring bar. Approximately 40 mL of THF was added, which immediately produced a green solution. After the mixture was stirred overnight, the solvent was removed under vacuum to leave a green solid. Hexanes (20 mL) was added, and insoluble impurities were removed by filtration over a medium-porosity glass frit. The solvent was removed from the green filtrate by slow evaporation; after 48 h, large hexagonally shaped crystals were isolated by decanting the remaining mother liquor. The solvent was evaporated from the latter under vacuum to afford additional solid as a powder. Total yield: 0.101 g (35% yield). Characterization of the crystals, which were found to contain 0.25 molecule of hexane per chromium complex: mp 129−131 °C. Anal. Calcd for $C_{31.5}H_{49.5}CrSi_4$: C, 63.85; H, 8.42. Found: C, 63.77; H, 8.60. Principal IR bands (cm^{-1}): 3067 (m), 2997 (s), 2897 (m), 1600 (w), 1448 (m), 1403 (w), 1254 (s), 1020 (m), 938 (w), 841 (s), 760 (s), 689 (s), 615 (w), 470 (m). Solution magnetic moment ((μ (T (K)): 3.04 (183), 3.03 (193), 3.01 (203), 3.01 (213), 3.01 (223), 2.99 (233), 2.99 (243), 3.00 (253), 3.03 (263), 3.06 (273), 3.10 (283), 3.18 (293), 3.22 (300).

General Procedures for X-ray Crystallography. A suitable crystal of each sample was located, attached to a glass fiber, and mounted on a Siemens SMART system for data collection at 173(2) K. Data collection and structure solution for all molecules were conducted at the X-ray Crystallography Laboratory at the University of Minnesota. Data to a resolution of 0.84 Å were considered in the data reduction (SAINT 6.1, Bruker Analytical X-ray Systems, Madison, WI). The intensity data were corrected for absorption (SADABS[38]). Final cell constants were calculated from a set of strong reflections measured during the actual data collection. Relevant crystal and data collection parameters for each of the compounds are given in Table 1.

The space groups were determined from systematic absences and intensity statistics. A direct-methods solution (SIR92[39]) was calculated that provided most of the non-hydrogen atoms from the E-map. Several full-matrix least-squares/difference Fourier cycles (SHELXTL-Plus V5.10, Bruker Analytical X-ray Systems, Madison, WI) were performed that located the remainder of the non-hydrogen atoms. All non-hydrogen atoms were refined with anisotropic displacement parameters. All hydrogen atoms were placed in ideal positions and refined as riding atoms with relative isotropic displacement parameters. Special considerations required for the structure of $(Ind^{2Si})_2Cr$ are given below.

Crystallographic Details for $(Ind^{2Si})_2Cr\cdot 0.25\ C_6H_{14}$. The asymmetric unit consists of two independent molecules, which are related by pseudosymmetry, and a solvent molecule that is disordered over an inversion center in a channel along [*a*,0.5,0.5]. The space group $P2_1/c$ was determined as specified in the general procedures. A number of reflections, however, violate the extinction condition for a *c*-glide and indicate the presence of an *a*-glide. Considering the latter, an attempt was made to solve the structure in the nonstandard setting $P2_1/a$; this effort failed, suggesting that the *a*-glide is a pseudosymmetry element. The two pseudosymmetrically related molecules were refined with a strong set of restraints and constraints; e.g., the 1,2 and 1,3 distances as well as the displacement parameters were refined to be similar within a given standard deviation. The solvent molecule was constrained to have ideal geometry (distances and bond angles).

Computational Details. Molecular mechanics calculations used the MMFF94 force field as implemented in PC Spartan Pro.[40] Both density functional theory (DFT) and extended Hückel (EHT) calculations were used to investigate the staggered and gauche forms of Ind_2Cr. Despite the well-known limitations of the EHT method,[41] it can provide qualitatively correct orbital energy ordering and offers a convenient way to visualize orbital interactions. Density functional theory calculations were performed using the Gaussian 98W program.[42] Geometry optimizations of the Ind_2Cr system were performed with the B3PW91

(38) Blessing, R. H. *Acta Crystallogr.* **1995**, *A51*, 33−38.
(39) Altomare, A.; Cascarno, G.; Giacovazzo, C.; Gualardi, A. *J. Appl. Crystallogr.* **1993**, *26*, 343−350.
(40) PCSpartanPro **1999**, PC Spartan Pro 1.1, Wavefunction, Inc. Irvine, CA.
(41) Whangbo, M.-H. *Theor. Chem. Acc.* **2000**, *103*, 252−256.
(42) *Gaussian 98* (Revision A.7); Frisch, M. J.; Trucks, G. W.; Schlegel, H. B.; Scuseria, G. E.; Robb, M. A.; Cheeseman, J. R.; Zakrzewski, V. G.; Montgomery, J. A.; Stratmann, R. E.; Burant, J. C.; Dapprich, S.; Millam, J. M.; Daniels, A. D.; Kudin, K. N.; Strain, M. C.; Farkas, O.; Tomasi, J.; Barone, V.; Cossi, M.; Cammi, R.; Mennucci, B.; Pomelli, C.; Adamo, C.; Clifford, S.; Ochterski, J.; Petersson, G. A.; Ayala, P. Y.; Cui, Q.; Morokuma, K.; Malick, D. K.; Rabuck, A. D.; Raghavachari, K.; Foresman, J. B.; Cioslowski, J.; Ortiz, J. V.; Stefanov, B. B.; Liu, G.; Liashenko, A.; Piskorz, P.; Komaromi, I.; Gomperts, R.; Martin, R. L.; Fox, D. J.; Keith, T.; Al-Laham, M. A.; Peng, C. Y.; Nanayakkara, A.; Gonzalez, C.; Challacombe, M.; Gill, P. M. W.; Johnson, B. G.; Chen, W.; Wong, M. W.; Andres, J. L.; Head-Gordon, M.; Replogle, E. S.; Pople, J. A. Gaussian, Inc., Pittsburgh, PA, 1998.

Table 1. Crystal Data and Summary of X-ray Data Collection

compound	$(Ind^{1T})_2Cr$	$(Ind^{2T})_2Cr$	$(Ind^{2Si})_2Cr$
formula	$C_{26}H_{30}Cr$	$C_{34}H_{46}Cr$	$C_{31.5}H_{49.5}CrSi_4$
formula weight	394.50	506.71	592.57
color of cryst	violet	brick red	jade green
cryst dimens, mm	0.12 × 0.10 × 0.06	0.31 × 0.25 × 0.24	0.25 × 0.19 × 0.05
space group	$P2_1/n$	$P2_1/c$	$P2_1/c$
cell dimens (173(2) K)			
a, Å	9.7902(11)	18.260(7)	11.098(1)
b, Å	10.9413(13)	9.694(4)	16.192(2)
c, Å	10.6855(12)	17.921(7)	38.358(4)
β, deg	113.714(2)	115.893(6)	92.973(2)
volume, Å^3	1048.0(2)	2853.6(18)	6883.6(11)
Z	2	4	8
calcd density, Mg/m^3	1.250	1.179	1.144
abs coeff, mm^{-1}	0.553	0.420	0.490
F(000)	420	1,096	2,548
radiation type	Mo *K*α (0.710 73 Å)	Mo *K*α (0.710 73 Å)	Mo *K*α (0.710 73 Å)
temperature, K	173(2)	173(2)	173(2)
limits of data collection	$2.39° \le \theta \le 27.54°$	$2.28° \le \theta \le 27.48°$	$1.37° \le \theta \le 25.06°$
index ranges	$-12 \le h \le 11$, $0 \le k \le 14$, $0 \le l \le 13$	$-22 \le h \le 23$, $-11 \le k < 12$, $-22 \le l \le 22$	$-13 \le h \le 13$, $-19 \le k \le 10$, $-45 \le l \le 45$
total reflcns collected	9,328	18,522	38,919
no. of unique reflcns	2388 ($R_{int} = 0.0327$)	6458 ($R_{int} = 0.0750$)	12 158 ($R_{int} = 0.0571$)
weighting scheme[a]	$A = 0.041$, $B = 0.0$	$A = 0.0718$, $B = 0.0$	$A = 0.0604$, $B = 41.307$
transmn factors	1.000−0.826	1.000−0.691	1.000−0.773
data/restraints/params	2388/0/127	6458/0/374	12 158/364/672
R indices ($I>2\sigma(I)$)	$R = 0.0369$, $R_w = 0.0833$	$R = 0.0469$, $R_w = 0.1160$	$R = 0.0830$, $R_w = 0.1946$
R indices (all data)	$R = 0.0677$, $R_w = 0.0885$	$R = 0.0644$, $R_w = 0.1267$	$R = 0.1178$, $R_w = 0.2096$
goodness of fit on F^2	0.985	0.986	1.072
max/min peak in final diff map, e$^-$/Å^3	0.269/−0.287	0.430/−0.513	1.212/−1.579

[a] $w = [\sigma^2(F_o^2) + (AP)^2 + (BP)]^{-1}$, where $P = (F_o^2+2F_c^2))/3$.

functional[43,44] and the LANL2DZ basis set; the latter comprises the D95 Dunning/Huzinaga full double-ζ basis on first-row atoms,[45] and the Los Alamos ECP plus DZ on heavier atoms.[46] EHT calculations were performed with HyperChem Release 6, using an unweighted Hückel constant of 1.75 and previously described parameters for chromium.[47] The geometries derived from the DFT optimizations were used as input for single-point energy EHT calculations.

Results

Ligand and Complex Synthesis. Indene is easily deprotonated with an equivalent of *n*-BuLi in hexanes, and the resulting lithium indenide will react with an alkyl halide to afford a monosubstituted indene.[36] The latter can be deprotonated with an additional equivalent of *n*-BuLi, and its reaction with another equivalent of an alkyl halide leads to the isolation of disubstituted indenes.[37] The indenes used in this study were readily deprotonated by *n*-BuLi or $K[N(SiMe_3)_2]$ in hexanes or toluene, and the resulting air-sensitive salts were isolated in moderate to high yield.

Bis(indenyl)chromium(II) complexes were formed by salt elimination/metathesis reactions. Two equivalents of an indenyl salt was allowed to react with $CrCl_2$ in THF. Following the removal of THF under vacuum, a minimal amount of hexanes served to extract the chromium complexes, allowing for the removal of the alkali metal chloride byproducts. The purified bis(indenyl)chromium complexes were crystallized either by slow evaporation of a saturated solution or by cooling of a concentrated solution to approximately −30 °C.

Solution Magnetic Susceptibility Measurements. A variable-temperature magnetic susceptibility study in solution was performed on each compound. The complexes formed with monosubstituted indenes contain a high-spin metal center. $(Ind^{1T})_2Cr$ and $(Ind^{1Si})_2Cr$ display magnetic moments in solution ($\mu_B = 4.8$ and 4.9, respectively) from room temperature down to ∼183 K that essentially match the spin-only value for four unpaired electrons (4.90 μ_B). They behave similarly to the isopropyl-substituted $(Ind^{2i})_2Cr$.[27]

The magnetic properties of the disubstituted indenyl chromium complexes are substantially different from that of their monosubstituted counterparts. The bis(trimethylsilyl)-substituted indene complex ($(Ind^{2Si})_2Cr$) is clearly low spin ($\mu_B = 3.0-3.2$; cf. $\mu_B = 2.83$ for two unpaired electrons) in solution over a broad range of temperatures (183−300 K). The *t*-Bu analogue behaves in a distinctive way; above 300 K, solutions of $(Ind^{2T})_2Cr$ are brick red and have a μ_B of 3.6 (av). As the temperature drops, the solutions turn green, and μ_B gradually decreases to 2.9 (av) below 213 K.

Solid-State (SQUID) Magnetic Susceptibility Measurements. Three samples were selected for more detailed examination of their magnetic properties in the solid state. The magnetic moment displayed by $(Ind^{1Si})_2Cr$ indicates that it is high spin down to 30 K in the solid state. Above 30 K, the effective magnetic moment (4.1) is somewhat lower than the spin-only value for four unpaired electrons, but it remains unchanged up to 275 K. It is comparable to the value observed for high-spin $(Ind^{2i})_2Cr$.[27]

Paralleling its behavior in solution, $(Ind^{2Si})_2Cr$ is almost completely low spin in the solid state from liquid He temperatures up to 300 K; the magnetic moment from 10 to 150 K averages 2.8 μ_B, equal to the spin-only value for two unpaired

(43) Becke, A. D. *J. Chem. Phys.* **1993**, *98*, 5648−5652.
(44) Perdew, J. P.; Wang, Y. *Phys. Rev. B* **1992**, *45*, 13244−13249.
(45) Dunning, T. H., Jr.; Hay, P. J. In *Modern Theoretical Chemistry*; Schaefer, H. F., III, Ed.; Plenum: New York, 1976; pp 1−28.
(46) Wadt, W. R.; Hay, P. J. *J. Chem. Phys.* **1985**, *82*, 284−298.
(47) Stowasser, R.; Hoffmann, R. *J. Am. Chem. Soc.* **1999**, *121*, 3414−3420.

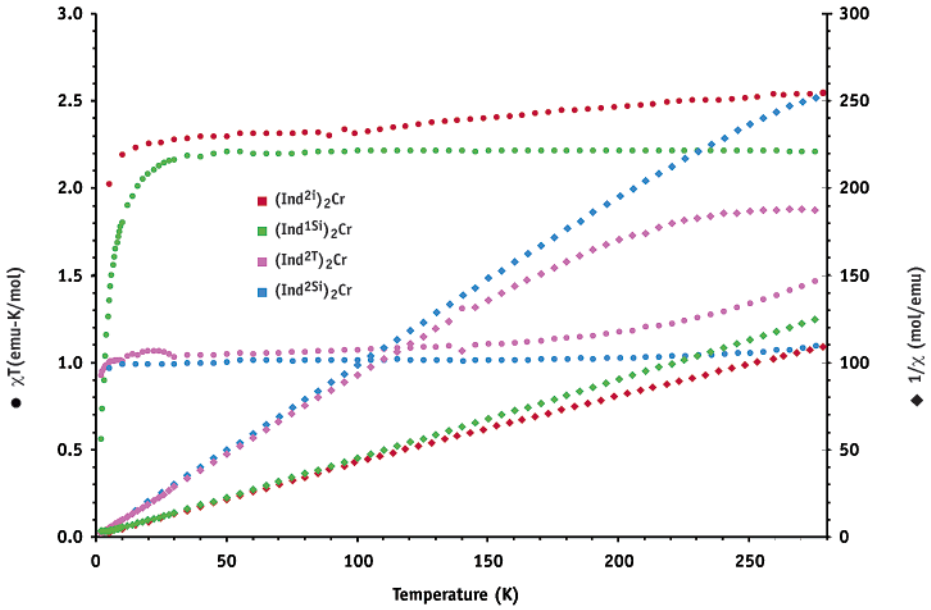

Figure 2. Plots of χT (circles) and $1/\chi$ (diamonds) for $(Ind^{1Si})_2Cr$, $(Ind^{2T})_2Cr$, $(Ind^{2Si})_2Cr$, and $(Ind^{2i})_2Cr$. Data for $(Ind^{2i})_2Cr$ are taken from ref 27.

electrons. There is some evidence that the compound is beginning a spin transition above 250 K, but even at 350 K, μ_B is only 3.3. Below 120 K, $(Ind^{2T})_2Cr$ is also low spin and possesses the magnetic moment ($\mu_B = 2.8$) appropriate for two unpaired electrons. Above this temperature, the effective magnetic moment begins to rise and reaches 3.4 by 275 K.

Plots of χT and $1/\chi$ for three of the new compounds and $(Ind^{2i})_2Cr$ are given in Figure 2. The complexes display simple Curie law behavior below 125 K, although their properties differ somewhat as the temperature is increased. For $(Ind^{1Si})_2Cr$, Curie law behavior continues to 275 K, and the near-zero slope of χT versus temperature is consistent with the absence of a spin-state change. A small amount of zero-field splitting is evident below 30 K. $(Ind^{2Si})_2Cr$ also displays some zero-field splitting below 20 K, but above 125 K, the slope of χT begins to increase and deviates from Curie law behavior. Any indications of a transition to a higher spin state are inconclusive, however. The χT value of 1.35 even at 350 K (not shown on the graph) is still considerably beneath the values found in high-spin $(Ind^{2i})_2Cr$ and $(Ind^{1Si})_2Cr$ (2.5 and 2.2, respectively) at 275 K. For $(Ind^{2T})_2Cr$, a small amount of zero-field splitting is found below 20 K, and as with $(Ind^{2Si})_2Cr$, the slope of χT begins to increase and deviate from Curie law behavior above 125 K. The χT value at 275 K (1.4) is slightly higher than that found in $(Ind^{2Si})_2Cr$ (1.1 at 275 K) but is still considerably beneath the values found in high-spin $(Ind^{2i})_2Cr$ and $(Ind^{1Si})_2Cr$.

Solid-State Structures. $(Ind^{1T})_2Cr$. Crystals of $(Ind^{1T})_2Cr$ were obtained from cold hexanes as purple blocks. Two indenyl ligands flank the metal center in a staggered meso configuration, with the *tert*-butyl groups aligned on opposite sides of the metal. Only half of the molecule is unique, as the metal lies on an inversion center. We have no evidence for the existence of other possible conformations of the molecule (e.g., an eclipsed meso form). An ORTEP of the compound is provided in Figure 3, displaying the numbering scheme used in the text; selected bond lengths and angles are given in Table 2.

The average Cr−C ring distance (2.32(4) Å) is indicative of a high-spin chromium(II) center; it is identical to that found in high-spin $(Ind^{2i})_2Cr$ (2.32(2) Å)[27] and is substantially longer than that in low-spin $Ind^*{}_2Cr$ (2.18(2) Å).[26] The bridgehead Cr−C contacts (av 2.404(3) Å) are longer than the Cr−C distances for C1, C2, and C3 (av 2.262(3) Å), but the range of the Cr−C ($\Delta = 0.14$ Å) bonds is similar to that found in both $(Ind^{2i})_2Cr$ ($\Delta = 0.14$ Å) and $Ind^*{}_2Cr$ ($\Delta = 0.10$ Å). A small degree of slippage is typical for indenyls bound to transition

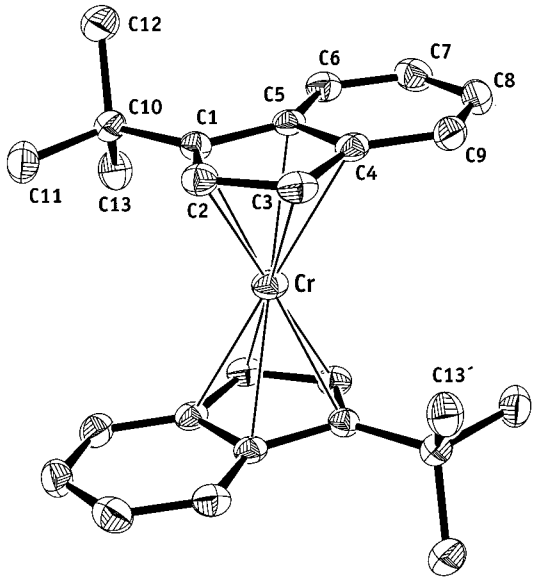

Figure 3. ORTEP drawing of the non-hydrogen atoms of $(Ind^{1T})_2Cr$, giving the numbering scheme used in the text. Thermal ellipsoids are shown at the 50% level.

Table 2. Selected Bond Distances (Å) and Angles (deg) for $(Ind^{1T})_2Cr$

atoms	distance	atoms	distance
Cr(1)−C(1)	2.285(2)	Cr(1)−C(4)	2.395(2)
Cr(1)−C(2)	2.252(2)	Cr(1)−C(5)	2.413(2)
Cr(1)−C(3)	2.249(2)	C(3)···C(13)	3.72
Cr(1)-centroid	1.968		
displacement of *t*-Bu group from ring plane 0.068			
ring centroid-Cr(1)-ring centroid 180			

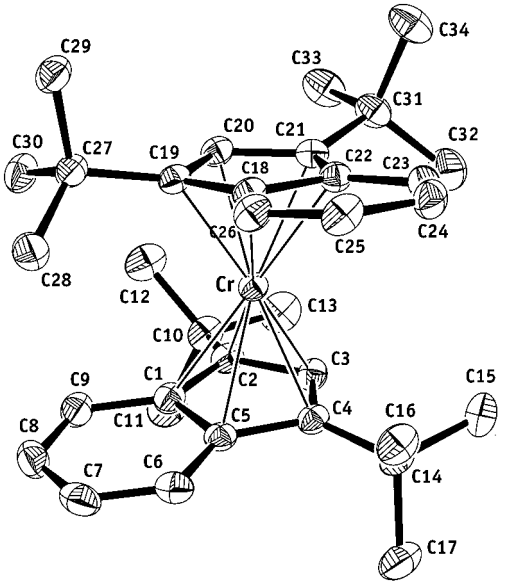

Figure 4. ORTEP drawing of the non-hydrogen atoms of $(Ind^{2T})_2Cr$, giving the numbering scheme used in the text. Thermal ellipsoids are drawn at the 50% level.

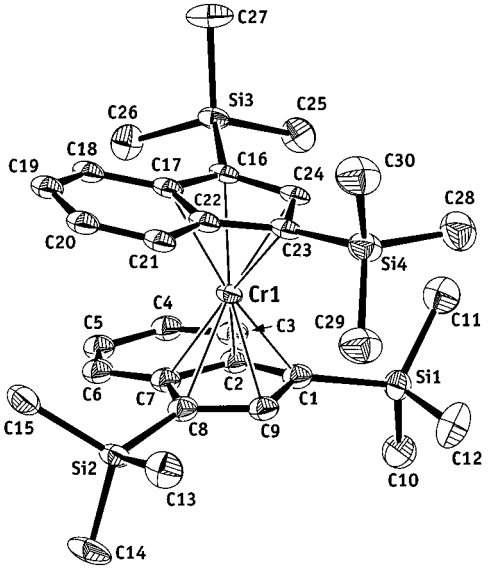

Figure 5. ORTEP drawing of one of the independent molecules of $(Ind^{2Si})_2Cr$, giving the numbering scheme used in the text. Thermal ellipsoids are shown at the 50% level.

Table 3. Selected Bond Distances (Å) and Angles (deg) for $(Ind^{2T})_2Cr$

atoms	distance	atoms	distance
Cr(1)−C(1)	2.297(2)	Cr(1)−C(18)	2.3070(19)
Cr(1)−C(2)	2.1901(19)	Cr(1)−C(19)	2.174(2)
Cr(1)−C(3)	2.138(2)	Cr(1)−C(20)	2.129(2)
Cr(1)−C(4)	2.188(2)	Cr(1)−C(21)	2.196(2)
Cr(1)−C(5)	2.2989(19)	Cr(1)−C(22)	2.3086(19)
Cr(1)-cent(C1−C5)	1.855(3)	Cr(1)-cent(C18−C22)	1.855(3)
av displacement of *t*-Bu group from ring plane 0.253			
ring centroid-Cr(1)-ring centroid 175.5			

metals and should not be interpreted as $\eta^5 \rightarrow \eta^3$ indenyl ring slippage for $\Delta < 0.3$.[48]

Like $(Ind^{2i})_2Cr$, $(Ind^{1T})_2Cr$ does not exhibit any noticeably close contacts between the ligands. It is not surprising, however, that the shortest C−C contact found in $(Ind^{1T})_2Cr$ is between C3 and C13′ (3.71 Å) and is closer than the smallest value (3.80 Å) in $(Ind^{2i})_2Cr$, as a methyl group must be pointed toward the opposite ligand in $(Ind^{1T})_2Cr$. *tert*-Butyl groups cannot avoid this contact, but isopropyl groups can rotate so that a hydrogen atom points toward the opposite ligand, thereby minimizing steric repulsion.

$(Ind^{2T})_2Cr$. Crystals of $(Ind^{2T})_2Cr$ were obtained as red blocks by allowing a hexanes solution to evaporate slowly. Unlike the geometry found in $(Ind^{1T})_2Cr$, the rings are in a gauche rather than a staggered arrangement around the central Cr(II); the twist angle is 87.1°. An ORTEP drawing is provided in Figure 4, displaying the numbering scheme used in the text; selected bond lengths and angles are given in Table 3.

The Cr−C ring distance (av 2.22(2) Å) is indicative of a low-spin chromium(II) center; it is similar to that found in low-spin $Ind^*{}_2Cr$[26] (2.18(2) Å) and in low-spin chromocenes (cf. 2.151(4) Å in $(C_5H_5)_2Cr$,[49] 2.17(1) Å in $[1,2,4\text{-}C_5(i\text{-}Pr)_3H_2]_2Cr$,[50] and 2.197(5) Å in $(C_5Ph_4H)_2Cr$).[51] It is significantly shorter than that observed in the high-spin complexes $(Ind^{2i})_2Cr$ (2.32(2) Å)[27] and $(Ind^{1T})_2Cr$ (2.32(4) Å). The closest contact between the *tert*-butyl groups is 3.96 Å, which is equal to the sum of the van der Waals radii for two methyl groups.[52] Both rings are η^5-bound to the chromium; the range ($\Delta = 0.12$ Å) is similar to values found for $(Ind^{1T})_2Cr$ ($\Delta = 0.14$ Å), $(Ind^{2i})_2Cr$ ($\Delta = 0.14$ Å),[27] and $Ind^*{}_2Cr$ ($\Delta = 0.10$ Å).[26] The indenyl ligands are noticeably canted, with an interplanar angle of 171.8°. The existence of some steric crowding in the molecule is evident by the displacement of the *t*-Bu groups from the C_5 ring plane; it averages to 0.25 Å, with a maximum value of 0.34 Å for C(31). This is distinctly larger than the corresponding alkyl group displacements in high-spin $(Ind^{2i})_2Cr$ (0.079 Å) or low-spin $[1,2,4\text{-}C_5(i\text{-}Pr)_3H_2]_2Cr$ (0.10 Å).[50] The C_6 ring forms an angle of 2.9° with the C_5 ring plane; this is appreciably more than in $(Ind^{2i})_2Cr$ (1.3°) or $(Ind^{1T})_2Cr$ (0.58°).[53]

$(Ind^{2Si})_2Cr$. Crystals of $(Ind^{2Si})_2Cr$ were isolated as dark green hexagonal plates by allowing a hexanes solution to evaporate slowly. There are two independent, but essentially identical molecules related by pseudosymmetry in the unit cell; a solvent molecule is also incorporated into the lattice. The geometry is similar to that found in $(Ind^{2T})_2Cr$; the rings are in a gauche arrangement (twist angles of 86.3° and 86.8°) around the central chromium. As the two molecules are similar, the rest of the discussion will focus on the one containing Cr(1). An ORTEP drawing of the molecule is provided in Figure 5, displaying the numbering scheme used in the text; selected bond lengths and angles are given in Table 4.

The Cr−C ring distance (av 2.20(2) Å) is indicative of a low-spin chromium(II) center. It is similar to that in low-spin $Ind^*{}_2Cr$[26] (2.18(2) Å) and $(Ind^{2T})_2Cr$ (2.22(2) Å) and is slightly

(48) Faller, J. W.; Crabtree, R. H.; Habib, A. *Organometallics* **1985**, *4*, 929−935.
(49) Flower, K. R.; Hitchcock, P. B. *J. Organomet. Chem.* **1996**, *507*, 275−277.
(50) Overby, J. S.; Schoell, N. J.; Hanusa, T. P. *J. Organomet. Chem.* **1998**, *560*, 15−19.
(51) Castellani, M. P.; Geib, S. J.; Rheingold, A. L.; Trogler, W. C. *Organometallics* **1987**, *6*, 1703−1712.
(52) Pauling, L. *The Nature of the Chemical Bond*, 3rd ed.; Cornell University Press: Ithaca, NY, 1960.
(53) The crystal structure of $(Ind^{2T})_2Cr$ has been described in a review article (Sitzmann, H. *Coord. Chem. Rev.* **2001**, *214*, 287−327). Some properties mentioned for the compound (i.e., "deep purple", "high-spin") appear to differ from our findings.

Table 4. Selected Bond Distances (Å) and Angles (deg) for $(Ind^{2Si})_2Cr$

atoms	distance	atoms	distance
Cr(1)−C(1)	2.167(6)	Cr(2)−C(31)	2.157(6)
Cr(1)−C(2)	2.268(6)	Cr(2)−C(32)	2.260(6)
Cr(1)−C(7)	2.285(6)	Cr(2)−C(37)	2.287(6)
Cr(1)−C(8)	2.189(6)	Cr(2)−C(38)	2.145(6)
Cr(1)−C(9)	2.113(6)	Cr(2)−C(39)	2.113(6)
Cr(1)-cent(C1−C9)	1.831	Cr(2)-cent(C31−C39)	1.820
Cr(1)−C(16)	2.161(6)	Cr(2)−C(46)	2.177(6)
Cr(1)−C(17)	2.277(6)	Cr(2)−C(47)	2.283(6)
Cr(1)−C(22)	2.265(6)	Cr(2)−C(52)	2.268(6)
Cr(1)−C(23)	2.163(6)	Cr(2)−C(53)	2.171(6)
Cr(1)−C(24)	2.102(6)	Cr(2)−C(54)	2.116(6)
Cr(1)-cent(C16−C24)	1.822	Cr(2)-cent(C46−C54)	1.832
av displacement of *t*-Bu group from ring plane 0.31			
ring centroid-Cr(1)-ring centroid 170.0			

more than 0.1 Å shorter than that in the high-spin $(Ind^{2i})_2Cr$ (2.32(2) Å)[27] and $(Ind^{1T})_2Cr$ (2.32(4) Å). As with other bis(indenyl) chromium(II) complexes, the rings are η^5-bound to the chromium and exhibit a range ($\Delta_{Cr-C} = 0.18$ Å) that is similar to, although slightly larger than, values found in low-spin $(Ind^{2T})_2Cr$ ($\Delta = 0.12$ Å) and $Ind^*{}_2Cr$ ($\Delta = 0.10$ Å). This compound is also bent, with an angle between the two C_5 planes of 11.5°, which is even larger than the 8.2° found in $(Ind^{2T})_2Cr$.

The trimethylsilyl groups are also markedly displaced from the C_5 ring plane by an average of 0.31 Å, with a maximum value of 0.42 Å; this represents an increase over that of the di-*tert*-butyl derivative by 0.054 Å. The C_6 rings form an angle with the C_5 ring planes of 3.8° (av), which is noticeably more than in $(Ind^{2i})_2Cr$ (1.6°), $(Ind^{1T})_2Cr$ (0.58°), and even $(Ind^{2T})_2Cr$ (2.9°).

Sterically Directed Ligand Rotation. Comparison of the structures of $(Ind^{2T})_2Cr$ and $(Ind^{2Si})_2Cr$ with that of $(Ind^{2i})Cr$[27] suggests that the *t*-Bu and $SiMe_3$ groups exert a marked effect on the conformations of the indenyl ligands. To obtain an estimate of the size of this effect, molecular mechanics calculations using the MMFF94 force field were performed on $(Ind^{2T})_2Cr$ and $(Ind^{2Si})_2Cr$. An initial metal−ring centroid distance constraint of 1.98 Å was used, which is a typical value for high-spin bis(indenyl)chromium species. The calculated strain energy drops on rotating from a staggered to a gauche conformation by 8.2 and 6.1 kcal mol^{-1} for $(Ind^{2T})_2Cr$ and $(Ind^{2Si})_2Cr$, respectively. The calculated minimum rotation angles are 84.9° and 85.3° for the two complexes; these angles are not far from the crystallographically observed values of ∼87°. With a group less bulky than *t*-Bu or $SiMe_3$, there is little change in steric energy on rotation; the difference between the strain energy of $(Ind^{2i})_2Cr$ at 180° and its minimum energy conformation (63.1° rotation), for example, is a negligible 0.3 kcal mol^{-1}. It seems to be the case, therefore, that the gauche conformations of $(Ind^{2T})_2Cr$ and $(Ind^{2Si})_2Cr$ are directed by the bulk of the ring substituents.

Orbital Interactions in Staggered Ind_2Cr. High-spin, staggered Ind_2Cr was investigated with DFT methods. Attempts to optimize its structure under C_{2h} symmetry were unsuccessful, but the geometry converged under C_i symmetry, which was found to be a minimum on the potential energy surface ($N_{imag} = 0$). The optimized structure (B3PW91/LANL2DZ) has an average Cr−C bond length of 2.315 Å, which corresponds well with the structurally characterized examples (2.32 Å). The slip parameter value ($\Delta = 0.31$ Å) is somewhat larger than found in the other high-spin molecules (∼0.10−15 Å) but still indicates η^5-bonding to both ligands.

The interaction of transition metal d orbitals with the π orbitals of the indenyl anion has been described for eclipsed (ideally C_{2v}-symmetric)[54] and fully staggered (ideally C_{2h}-symmetric)[26] conformations. In the latter case, which is applicable to the high-spin bis(indenyl)chromium complexes discussed here, the a_u and b_u symmetry combinations of the indenyl π orbitals cannot interact with the d orbitals. A qualitative MO diagram for staggered Ind_2Cr (Figure 6) was constructed from EHT calculations, using the coordinates from the DFT-optimized geometry. The *z* axis is taken as perpendicular to the five-membered rings, which underscores the relationship of the indenyl interactions to those in metallocenes. The labeling of the π orbitals of the indenyl anion is the same as that used by previous authors,[54] with π_5 being the HOMO. Given the symmetry constraints on the molecule, it is not surprising that the MO diagram is qualitatively similar to that proposed for staggered, low-spin $Ind^*{}_2Cr$,[34] with some shifts in the energy levels of the frontier orbitals.

The HOMO of the complex is an antibonding combination of d_{xz} and π_4, with the next three filled orbitals being primarily metal-centered. The a_u and b_u combinations of the π_4 and π_5 orbitals are essentially nonbonding, and the electrons in the ligand π_3 orbitals display limited interaction with the metal 3d orbitals owing to their relative energy differences.

Orbital Interactions in Gauche Ind_2Cr. When the indenyl ligands in an Ind_2M complex are rotated to a gauche conformation, the molecular point group is lowered to C_2. Greater mixing of the d orbitals can now occur with the π orbitals of the indenyl anion. The symmetric and antisymmetric combinations of both the indenyl HOMO ($\pi_5-\pi_5$) and HOMO-1 ($\pi_4-\pi_4$) orbitals are of the proper symmetry to mix with the metal $d_{x^2-y^2}$, d_{z^2}, and d_{xy} (A symmetry) and d_{yz}, d_{xz} (B symmetry) orbitals.

Low-spin, gauche Ind_2Cr was investigated with DFT methods. With the dihedral angle between the 4−9, 4′−9′ bonds fixed at 90°, the optimized structure (B3PW91/LANL2DZ) converged to an average Cr−C length of 2.228 Å ($\Delta = 0.15$ Å); these values are in reasonably good agreement with those found for the structurally characterized $(Ind^{2T})_2Cr$ and $(Ind^{2Si})_2Cr$. Interestingly, the angle between the indenyl rings is 167.9°, which is comparable to that found in $(Ind^{2T})_2Cr$ (171.8°) and $(Ind^{2Si})_2Cr$ (168.5°), evidence that the bending observed in the crystal structures is not generated by the *t*-Bu or $SiMe_3$ substituents.

Coordinates of the DFT-optimized geometry were employed as input to an EHT calculation that was used to generate a qualitative MO diagram for low-spin Ind_2Cr (Figure 7). Mixing of the d orbitals with the indenyl π orbitals now occurs that permits additional bonding interactions. This is most clearly seen in the case of the π_4 orbitals, which combine with a mixture of the d_{xz} and d_{yz} orbitals to form bonding orbitals 42b and 41b. The corresponding antibonding combinations are raised far above the energy of the d_{z^2} orbital, which has now become the HOMO. A similar effect happens with the π_5 orbitals, with MO 43b forming from a $\pi_5-(d_{xy} + d_{xz})$ combination. MO 44b appears to reflect mixing of the $d_{x^2-y^2}$ orbital with d_{xz}, although the wave function remains largely localized on the indenyl ligands.

(54) Crossley, N. S.; Green, J. C.; Nagy, A.; Stringer, G. *J. Chem. Soc., Dalton Trans.* **1989**, 2139−2147.

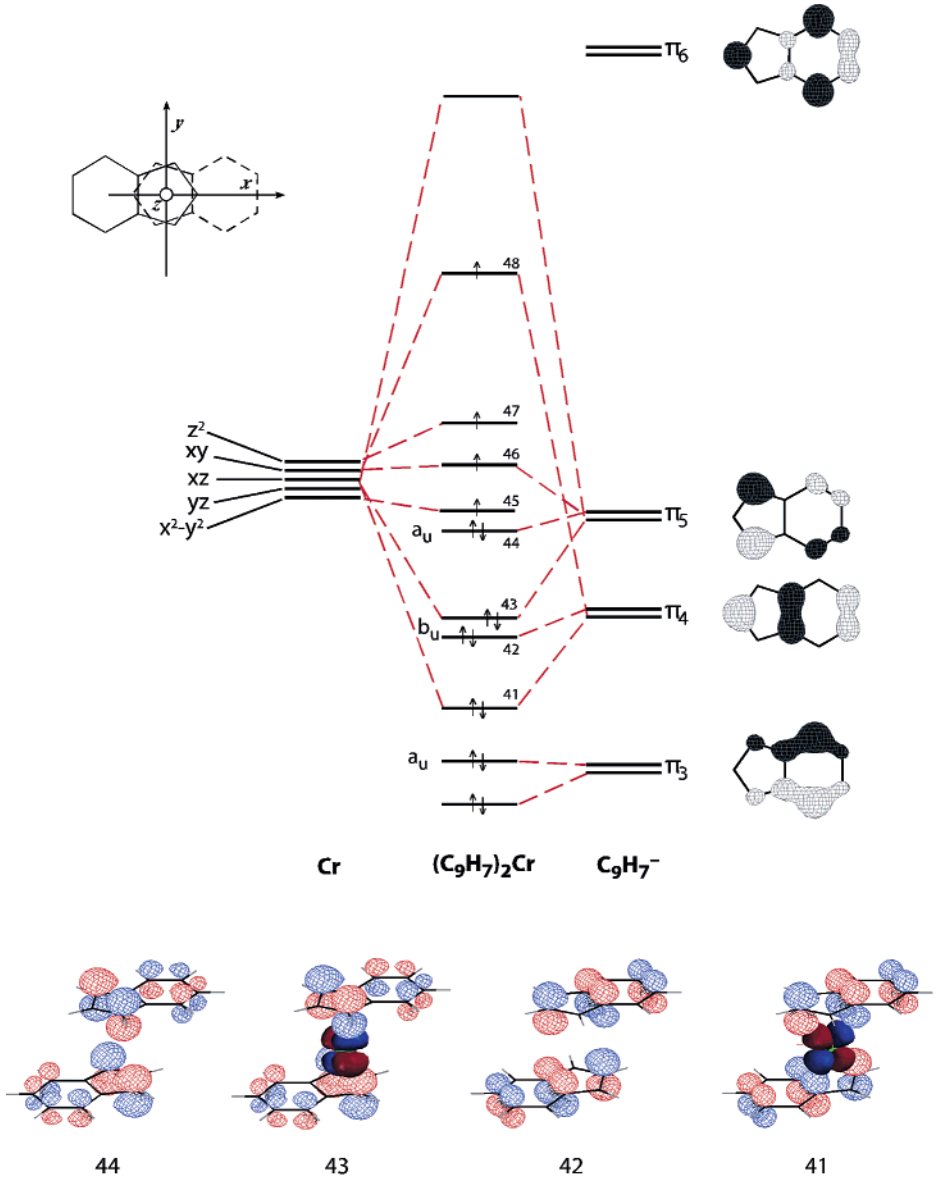

Figure 6. Qualitative MO diagram for high-spin, staggered Ind_2Cr. Energy levels were derived from extended Hückel calculations. Nonbonding orbitals 44 and 42 are forbidden by symmetry from interacting with the metal d orbitals.

Discussion

The chemistry of *indenyl* Cr(II) complexes can be paralleled to that of *cyclopentadienyl* Mn(II) species. For example, among the first-row metallocenes Cp_2M (M = V−Ni), only Cp_2Mn is not monomeric in the solid state. In the gas phase, however, Cp_2Mn exists as a monomer with a high-spin ($S = {}^5/_2$) electron configuration.[11] A similar pattern is found with bis(indenyl)-metal complexes (Ind_2M, M = V−Ni; Ind_2Mn is unknown); in this case, the chromium derivative is the one that is not monomeric. Computational analysis of Ind_2Cr suggests that if the staggered monomer were isolated, it would be a high-spin compound ($S = 2$). The high-spin states of the two chromium complexes with monosubstituted rings described here ($(Ind^{1Si})_2Cr$ and $(Ind^{1T})_2Cr$) and the previously characterized 1,3-disubstituted $(Ind^{2i})_2Cr$ [27] are fully consistent with the predicted spin state of staggered Ind_2Cr. The latter two compounds, which have been structurally authenticated, do not provide any evidence that intramolecular steric congestion is lengthening M−L distances to favor the high-spin state. Extending the indenyl/Cr and Cp/Mn analogy further, the permethylated complexes Cp^*_2Mn and Ind^*_2Cr are both low spin, and their magnetic state presumably reflects the strong donor properties of the heavily alkylated ligands.

The low-spin character of the two 1,3-disubstituted bis-(indenyl)chromium complexes containing *t*-Bu and $SiMe_3$ groups does not fit the pattern described above, however. The electronic properties of the two substituents do not explain the change in magnetic properties; the replacement of *i*-Pr by *t*-Bu, for example, should not alter the relative donor properties of the rings enough to favor low-spin complexes. In addition, the $SiMe_3$ group is known to be a net acceptor (e.g., it stabilizes the high-spin state of manganocenes[15]) and the addition of a second $SiMe_3$ group to the high-spin $(Ind^{1Si})_2Cr$ would not be likely to favor spin pairing if only inductive effects were operative.

Consequences of Imposed Ligand Rotation. The crystal structures of $(Ind^{2T})_2Cr$ and $(Ind^{2Si})_2Cr$ make it apparent that the *t*-Bu and $SiMe_3$ groups influence the structures of their

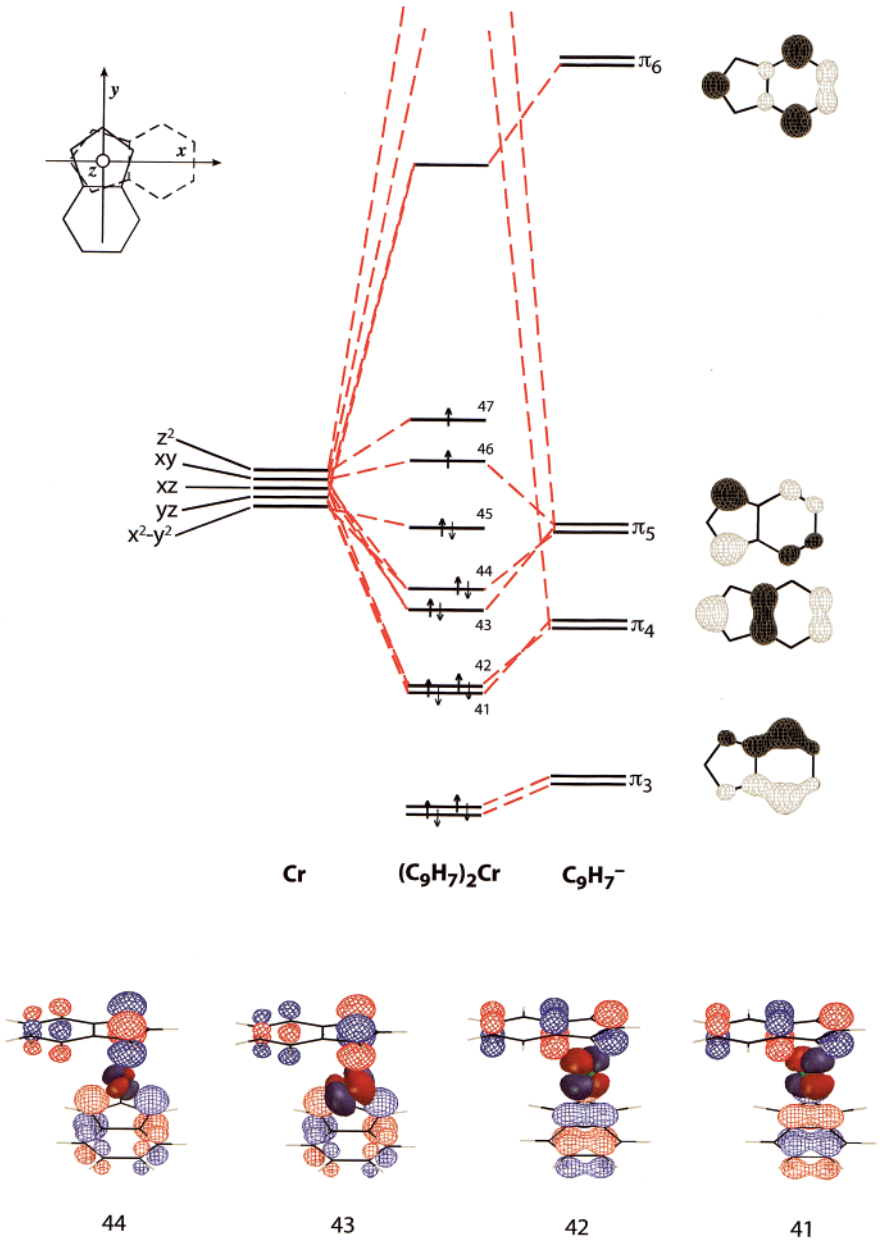

Figure 7. Qualitative MO diagram for low-spin, gauche Ind_2Cr. Energy levels were derived from extended Hückel calculations.

associated compounds through their steric bulk. Rotation of the indenyl ligands to a gauche (~90°) orientation relieves steric crowding, a fact supported by molecular mechanics calculations. In fact, in complexes with shorter M−indenyl distances than those found in the indenyl chromium compounds, gauche configurations are observed with even less bulky substituent groups; e.g., the complex $(Ind^{2i})_2Fe$, with an average Fe−C bond length of 2.068(7) Å, is gauche.[55]

Since the electron donor or acceptor properties of the substituted indenyl ligands are insufficient to explain the differences in the spin states of the complexes, the changes in metal−ligand interactions that accompany ligand rotation must be examined. The inversion symmetry of a staggered Ind_2M complex (C_{2h} or C_i) prohibits the interaction of ungerade combinations of the d orbitals with the ligand π orbitals. This restriction is removed under the lowered symmetry found in gauche configurations, and the resulting mixing of metal- and ligand-based orbitals provides bonding and antibonding orbitals that now lead to the low-spin state. The orientation of ligands in coordination compounds such as six-coordinate Fe(III) Schiff base and porphyrinate complexes is known to affect the spin states of the metal centers[56−59] (e.g., the effect of imidazole ring alignment on the magnetic properties of $[Fe(L)(HIm)_2]^+$ cations),[60] but the compounds described here represent the first organometallic sandwich structures in which enforced ligand orientation, rather than donation/inductive effects, appears to control the spin state of a complex.

(55) Overby, J. S.; Hanusa, T. P. Unpublished results.
(56) Kennedy, B. J.; McGrath, A. C.; Murray, K. S.; Skelton, B. W.; White, A. H. *Inorg. Chem.* **1987**, *26*, 483−495.
(57) Thuery, P.; Zarembowitch, J. *Inorg. Chem.* **1986**, *25*, 2001−2008.
(58) Nakamura, M.; Nakamura, N. *Chem. Lett.* **1991**, 1885−1888.
(59) Walker, F. A.; Simonis, U.; Zhang, H; Walker, J. M.; Ruscitti, T. M.; Kipp, C.; Amputch, M. A.; Castillo, B. V., III; Cody, S. H.; et al. *New J. Chem.* **1992**, *16*, 609−620.
(60) Hernandez-Molina, R.; Mederos, A.; Dominguez, S.; Gili, P.; Ruiz-Perez, C.; Castineiras, A.; Solans, X.; Lloret, F.; Real, J. A. *Inorg. Chem.* **1998**, *37*, 5102−5108.

It should be noted that gauche bis(indenyl) complexes are known in cases where steric effects do not appear to be driving the orientation. The $[Ind^*_2Cr]^+$ and $[Ind^*_2Co]^+$ cations are gauche (rotation angles of 89°), for example,[26] even though the neutral Ind^*_2Cr and Ind^*_2Co[61] compounds are staggered and eclipsed, respectively. The chromium-containing cation is a triplet, and it is not immediately apparent whether the charge and spin state are reflected in the ligand orientation. This may be a fruitful area for future study.

Conclusions

Accumulated evidence strongly supports the conclusion that monomeric Ind_2Cr, if isolated, would be a staggered, high-spin ($S = 2$) complex; this magnetic feature persists in the monosubstituted monomers $(Ind^{1T})_2Cr$ and $(Ind^{1Si})_2Cr$, and in the disubstituted $(Ind^{2i})_2Cr$. When the steric bulk of substituents in the 1,3 positions is increased beyond *i*-Pr, ligand rotation to a gauche (near 90°) conformation is forced upon the molecule. Owing to increased metal−ligand orbital mixing, maintenance of the high-spin state is no longer possible, and the molecules adopt low-spin configurations. This mechanism for spin-state alteration has not been observed in organometallic sandwich molecules before.

A low-spin state can also be imposed on a bis(indenyl)-chromium complex by the addition of sufficient alkyl groups to increase the donor strength of the molecule, as in Ind^*_2Cr. This suggests that both steric bulk and electronic effects brought about by selective substitution of the indenyl ligand could be used to tailor the magnetic properties of the compounds, making them suitable as readily tunable sources of variable-spin molecules. The marked geometric alterations associated with the spin-state changes also suggest that there may be useful variations in the reactivity of the complexes with donor ligands, a possibility we are investigating.

Acknowledgment. We thank Dr. Ron Goldfarb and the National Institute of Standards and Technology for the use of the SQUID magnetometers. We also express our appreciation to the Petroleum Research Fund, administered by the American Chemical Society, for partial support of this research (G.T.Y.).

Supporting Information Available: An X-ray crystallographic file in CIF format for $[1\text{-}(t\text{-Bu})C_9H_6]_2Cr$, $[1,3\text{-}(SiMe_3)_2\text{-}C_9H_5]_2Cr$, and $[1,3\text{-}(t\text{-Bu})_2C_9H_5]_2Cr$. This material is available free of charge via the Internet at http://pubs.acs.org. See any current masthead page for ordering information and Web access instructions.

JA012390A

(61) Westcott, S. A.; Kakkar, A. K.; Stringer, G.; Taylor, N. J.; Marder, T. B. *J. Organomet. Chem.* **1990**, *394*, 777−794.